The (1+1)DO(2) model: a finite lattice analysis

1988 J. Phys. A: Math. Gen. 21 2417

(http://iopscience.iop.org/0305-4470/21/10/019)

J. Phys. A: Math. Gen. **21** (1988) 2417-2429. Printed in the UK

The (1+1)D O(2) model: a finite lattice analysis

C R Allton and C J Hamer†

Department of Theoretical Physics, Research School of Physical Sciences, Australian National University, GPO Box 4, Canberra 2601, Australia

Received 10 November 1987

Abstract. Finite-size methods and the theory of conformal invariance are applied to the (1+1)D O(2) or X-Y planar model. The critical point is found to be $x_c \approx 2.0$, the value $\sigma = 0.501 \pm 0.005$ is obtained for the index governing the critical divergence of the correlation length and the conformal anomaly is confirmed to be $c = 1$. The Kosterlitz-Thouless features of a low-temperature phase with zero spontaneous magnetisation but algebraic decay of correlations, together with a standard high-temperature phase, are observed. The critical exponent η is determined as a function of coupling constant and compared with theoretical expectations.

1. Introduction

The O(2) or X-Y planar model is of special interest in statistical mechanics because of its unusual behaviour at the phase transition. The model has a standard high-temperature phase with an exponential decay of correlations, but it is believed to have an essential singularity in its correlation length ξ at a finite temperature or coupling g_c. In the low-temperature phase the correlations decay algebraically with separation, vanishing at infinite distances. Thus the model can be said to have a line of criticality for $g \leqslant g_c$.

A fundamental analytic study of the model has been performed by Kosterlitz and Thouless (1973). They hypothesised that the mechanism responsible for the transition was 'topological' in origin, being due to the unbinding of vortex-antivortex pairs. From a renormalisation analysis Kosterlitz (1974) obtained the following functional form for the correlation length:

$$\begin{aligned} \xi &\sim \exp\left[b\left(\frac{g_c}{g-g_c}\right)^{\sigma} \right] && g > g_c \\ &= \infty && g \leqslant g_c \end{aligned} \tag{1.1}$$

where $\sigma = \frac{1}{2}$. According to the standard connection between statistical mechanics and field theory the reciprocal of the correlation length ξ corresponds to the mass gap F of the equivalent quantum system.

Since then many analytical and numerical methods have been applied to try and confirm this structure, and estimate the critical coupling g_c and critical index η. Leaving aside much work on the 2D Euclidean model, these methods include high- and low-temperature series expansions (Hamer *et al* 1979, Hamber and Richardson 1981,

† Present address: Department of Theoretical Physics, School of Physics, University of New South Wales, PO Box 1, Kensington 2033, Australia.

0305-4470/88/102417+13$02.50

Luck 1982), finite lattice Hamiltonian approaches (Hamer and Barber 1981), Monte Carlo methods (see e.g. Fernández *et al* 1986, Heys and Stump 1984, Stump 1986) and some analytic work (Mattis 1984, Migdal 1975, Stump 1980).

In this paper our aim is to use a Hamiltonian finite-size scaling approach to determine the critical point and the critical exponent η as a function of coupling. We also test the application of conformal invariance to the system. Polyakov *et al* first introduced the hypothesis of conformal invariance to 2D statistical mechanics systems as criticality (Polyakov 1970, Belavin *et al* 1984a, b). Cardy has shown that these ideas of conformal invariance have special applicability to statistical systems of finite width and infinite length (strips). He argued that from the finite-size scaling amplitudes of the eigenvalues of the transfer matrix (or quantum Hamiltonian) one can determine (i) the universality class of the system (denumerated by the conformal anomaly c) and (ii) the system's critical exponents†. We apply this approach in § 3.3.

2. Method

The system can be realised as a Hamiltonian field theory on a one-dimensional lattice with a continuous time dimension (see Hamer *et al* 1979). In the angular momentum representation the M-site quantum Hamiltonian is

$$\tilde{\boldsymbol{H}} = \sum_{m=1}^{M} (\boldsymbol{J}^2(m) - \tfrac{1}{2}x\{\boldsymbol{J}_+(m)\boldsymbol{J}_-(m+1) + \boldsymbol{J}_-(m)\boldsymbol{J}_+(m+1)\} - \tfrac{1}{2}h\{\boldsymbol{J}_+(m) + \boldsymbol{J}_-(m)\}) \quad (2.1a)$$

$$= \boldsymbol{H}_0 - \tfrac{1}{2}x\boldsymbol{V} - \tfrac{1}{2}h\boldsymbol{W} \quad (2.1b)$$

with commutators

$$[\boldsymbol{J}(m), \boldsymbol{J}_\pm(m')] = \pm J_+(m)\delta_{m,m'} \quad (2.2)$$

where $\boldsymbol{J}(m)$ measures the spin at each site, $\boldsymbol{J}_\pm(m)$ is the raising/lowering operator, $x = 2/g^2$ (g is the temperature variable) and h is the magnetic coupling.

The finite lattice method we use to extract the energy eigenstates of the Hamiltonian is based on the work of Hamer and Barber (1981). The M-site Hamiltonian is represented on strong coupling ($x = 0$) basis states and the eigensolutions are obtained using a N-step nested Lanczos procedure‡.

The zero magnetic field Hamiltonian commutes with the total spin operator $\boldsymbol{S} = \Sigma_m \boldsymbol{J}(m)$, so the spectrum of eigenstates forms sectors labelled by the value of $\langle \boldsymbol{S} \rangle$. There are four eigenstates of interest to us: the ground and first excited states in the $\langle \boldsymbol{S} \rangle = 0$ sector (defined as $\|0\rangle\rangle$ and $\|2\rangle\rangle$ respectively) and the ground and first excited states in the $\langle \boldsymbol{S} \rangle = 1$ sector (defined as $\|1\rangle\rangle$ and $\|3\rangle\rangle$ respectively). These states have corresponding energies ω_i ($i = 0$ to 3). The mass gaps between states $\|i\rangle\rangle$ and $\|j\rangle\rangle$ are defined $F_{ij} = \omega_j - \omega_i$ ($i, j = 0$ to 3) with $F_{01} = F$.

2.1. *Cutoff schemes*

In the strong-coupling (angular momentum) representation each lattice spin can take on any integer value, so even the finite lattice Hamiltonian is infinite dimensional. A

† For the O(2) model, the connection between the mass gap scaling amplitude and the critical exponent η was actually proved by Luck (1982), in a low-temperature analysis which preceded Cardy's work.

‡ This Lanczos scheme is a generalisation of that of Berger *et al* (1977) where instead of forming a 2×2 matrix as an intermediate step an $N \times N$ matrix is formed. The most efficient value of N was found to be around 10.

further restriction on these configuration states is obviously required to make the finite-size model computationally tractable. Some possible truncation schemes have been discussed previously by Irving and Hamer (1983) and Patkós and Ruján (1985).

Three truncation schemes were investigated here. These imposed a limit on (i) order of formation, (ii) spin, and (iii) unperturbed energy of the strong-coupled basis states. The cutoff on the order of perturbation (scheme (i)) considers only those strong-couplng basis states formed up to the Nth order (see Irving and Hamer 1983). In scheme (ii) we restrict the spin at each site to that $|\langle \boldsymbol{J}(m)\rangle| \leq J_{\max}$ for all m, while in scheme (iii) the total unperturbed energy is restricted, $\langle \Sigma_m \boldsymbol{J}^2(m)\rangle \leq E^0_{\max}$.

The three cutoff schemes were applied to a six-site test lattice to find which was the most efficient: it turned out that the 'energy cutoff' method (scheme (iii)) gives the most accurate eigenvalues, around two orders of magnitude better than schemes (i) and (ii). For ferromagnetic spin models, one finds empirically that the amplitude of a strong-coupling basis state within the exact ground-state eigenvector tends to drop off exponentially with its unperturbed energy E^0; so this energy cutoff scheme, originally proposed by Irving and Hamer, is similar in effect to the importance sampling scheme of Patkós and Ruján, and is simpler to implement. Numerical details of the calculations are outlined in appendix 1, together with some notes on a more sophisticated scheme which attempted to take some account of basis states outside the cutoff, but was discarded because it was not cost-effective.

3. Results

3.1. Critical point

The first point of interest in the model lies in the determination of the critical point. We use three methods to find x_c:

(i) using finite-size scaling to determine where the mass gap scales as $1/M$ (see Hamer and Barber 1981);

(ii) fitting the numerically obtained Callan–Symanzik β function to the β function obtained from Kosterlitz's suggested form of the mass gap (inverse of (1.1)) (see Roomany and Wyld 1980); and

(iii) extrapolating the finite-size mass gaps directly to the bulk limit using the Romberg algorithm (this method follows that used by Beleznay (1986)).

3.1.1. Critical point from finite-size scaling of the mass gap. Following Hamer and Barber (1980) we define the mass gap ratio

$$R_M(x) = \frac{MF(x; M)}{(M-1)F(x; M-1)} \tag{3.1}$$

where $F(x; M)$ is the mass gap at coupling x and lattice size M; or introducing an 'M-shift':

$$R_M(x; \varepsilon) = \frac{(M+\varepsilon)F(x; M)}{(M-1+\varepsilon)F(x; M-1)}. \tag{3.2}$$

The pseudo-critical points x^*_M of the finite lattices are defined from $R_M(x^*_M; \varepsilon) = 1$. These form a sequence which extrapolate as $M \to \infty$ to the critical point x_c of the bulk model for any fixed value of ε.

The extrapolation is carried out on a number of different sequences of lattice sizes using the alternating M-shifted 'VBS algorithm' (Barber and Hamer 1982, Vanden Broeck and Schwartz 1979). The results for the sequences $M = 1, 2, \ldots, 7$ and $1, 2, \ldots, 9$ are plotted in figure 1. From this method we estimate $x_c = 1.9 \pm 0.1$. Another extrapolation routine, that of Lubkin (1952), generally did not give such consistent results.

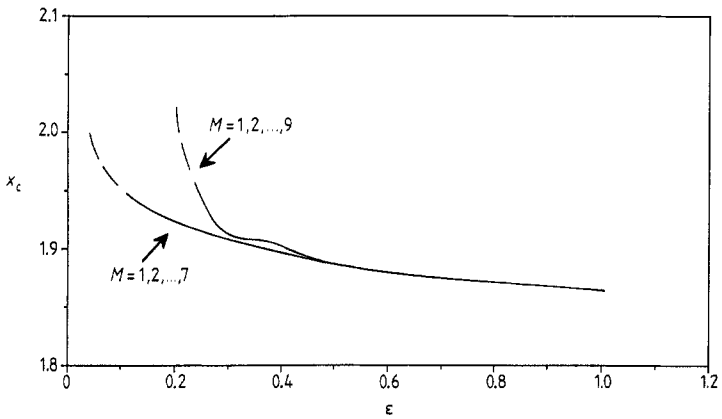

Figure 1. Critical point x_c against extrapolation parameter ε. These results are obtained using the alternating M-shifted VBS algorithm as described in § 3.1.1. The plots are from lattice sizes $M = 1, 2, \ldots, 7$ and $M = 1, 2, \ldots, 9$ as indicated. From this curve we estimate $x_c = 1.9 \pm 0.1$.

3.1.2. Using the Callan-Symanzik β function. The standard definition of the β function in terms of the mass gap is as follows (Hamer *et al* 1979):

$$\beta(x) = \frac{F(x)}{F(x) - 2xF'(x)}. \tag{3.3}$$

Substituting Kosterlitz's proposed functional form of the mass gap (the inverse of (1.1)) into (3.2) we obtain the following form of the β function for the O(2) model:

$$\beta(g)/g \sim (g - g_c)^{1+\sigma}. \tag{3.4}$$

The numerically obtained β function is fitted to this parametrised form.

A very useful finite-size Callan-Symanzik β function in terms of the finite-size mass gaps has been defined by Roomany and Wyld (1980):

$$\frac{\beta_M(g)}{g} = \left\{1 + \ln\left(\frac{F(x; M)}{F(x; M-1)}\right)\left[\ln\left(\frac{M}{M-1}\right)\right]^{-1}\right\} \times \left[1 - x\left(\frac{1}{F(x; M)}\frac{\partial F(x; M)}{\partial x} + \frac{1}{F(x; M-1)}\frac{\partial F(x; M-1)}{\partial x}\right)\right]^{-1}. \tag{3.5}$$

A numerical estimate of the bulk β function is obtained from extrapolating the finite-size $\beta_M(x)$ (3.5) to the $M = \infty$ limit. Again there is a choice of lattice sizes to use in the extrapolation sequence and a choice of extrapolating algorithms to use. We find the most consistent estimate of $\beta(g)$ is from the VBS algorithm using the lattice sizes $M = 1$

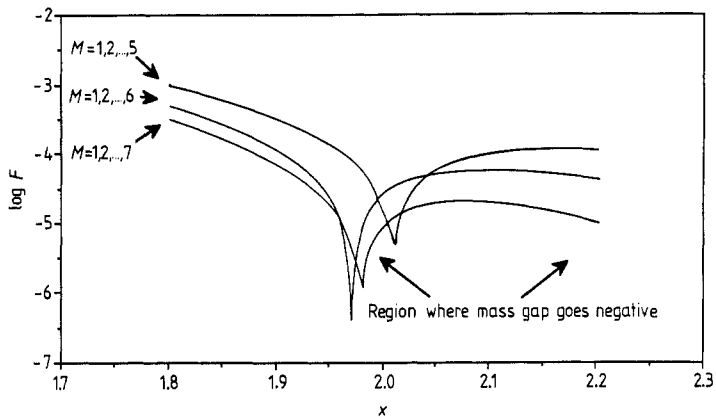

Figure 2. Log (base 10) of mass gaps from the Romberg extrapolation against coupling x plotted here for a variety of lattice sizes as shown. This approach is described in § 3.1.3. The mass gaps extrapolate to negative values in the region indicated. (In this region the log of the absolute value of the mass gaps is shown.)

to 8. We now fit this numerically obtained $\beta(g)$ to Kosterlitz's parametrised form (3.4) using a three-parameter least-squares fit and we obtain

$$x_c = 2.06 \pm 0.04 \tag{3.6a}$$

$$\sigma = 0.501 \pm 0.005. \tag{3.6b}$$

These compare favourably with values Kosterlitz obtained from his approximate solution of the model ($\sigma = \frac{1}{2}$) and agree with the results obtained by Roomany and Wyld using a similar fitting procedure.

3.1.3. Direct mass gap extrapolation via Romberg. This method follows that of Beleznay (1986). It employs the Romberg algorithm to extrapolate a sequence of finite-size mass gaps to the bulk limit assuming an expansion of the finite-size mass gaps in powers of $1/M$. Every possible combination of lattice sizes is used to form the sequence of mass gaps. (The Romberg algorithm can be applied to mass gaps from non-sequential lattice sizes.) Those sequences that converge give $x_c \approx 2.0$. The logarithms of the bulk mass gaps for a few sequences of lattice sizes ($M = 1, 2, \ldots, 5$; $M = 1, 2, \ldots, 6$ and $M = 1, 2, \ldots, 7$) are shown in figure 2. The Romberg algorithm also gives an upper bound for the error of the estimate. From this method using all the converging sequences of lattice sizes, we estimate $x_c = 2.00 \pm 0.03$. This confirms the results of Beleznay.

The three above estimates of x_c are comparable and give $x_c \approx 2.0$. The spread of results mirrors the subtlety of the transition.

3.2. The critical index η

For standard phase transitions the mass gap approaches zero as

$$F \sim (g - g_c)^{\nu} \tag{3.7}$$

in the vicinity of the critical point. However, since the mass gap for this model has an exponential form, ν itself cannot be defined. Similarly the exponents of the

magnetisation $\mathcal{M}$ and susceptibility χ (β and γ respectively) do not have standard definitions. However if $\mathcal{M}$ and χ are expressed in terms of the correlation length ξ one can make sensible definitions of related exponents $\tilde{\beta} = '\beta/\nu'$ and $\tilde{\gamma} = '\gamma/\nu'$ and continue to use finite-size scaling as usual,

$$\chi_M \sim \xi^{\tilde{\gamma}} \sim M^{\tilde{\gamma}} \qquad M \to \infty \tag{3.8a}$$

$$\mathcal{M}_M \sim \xi^{-\tilde{\beta}} \sim M^{-\tilde{\beta}} \qquad M \to \infty \tag{3.8b}$$

(see Kosterlitz 1974). The usual strong scaling laws give

$$\tilde{\gamma} = 2 - \eta \tag{3.9a}$$

$$\tilde{\beta} = \eta/2 \tag{3.9b}$$

so that the transition is effectively described by a single magnetic index η. The specific heat is not found to display any noticeable singularity.

We obtain the susceptibility χ from both

$$\chi_M = \frac{1}{M^2} \sum_{i=1}^{M} \sum_{m=1}^{M} \langle\langle 0 \| V(i, m) \| 0 \rangle\rangle \tag{3.10a}$$

where

$$V(i, m) = J_+(i)J_-(m) + J_-(i)J_+(m) \tag{3.10b}$$

(see Pesch and Kroemer 1985) and

$$\chi_M = \frac{-1}{M} \frac{\partial^2 \omega_0}{\partial h^2}\bigg|_{h=0} \tag{3.11}$$

(using the equivalence with statistical mechanics). We obtain the magnetisation $\mathcal{M}$ from:

$$\mathcal{M}_M = \frac{1}{M} \sum_{m=1}^{M} \langle\langle 1 \| J_+(m) + J_-(m) \| 0 \rangle\rangle \tag{3.12}$$

(see Hamer 1982). The exponent η can be determined from the χ_M and $\mathcal{M}_M$ ((3.10)-(3.12)) via the respective finite-size scaling relations $\chi_M \sim M^{2-\eta}$ and $\mathcal{M}_M \sim M^{-\eta/2}$ (using (3.8) and (3.9)). The best method we found for extracting the exponent from these scaling relations of the form $\Phi_M \sim M^{\alpha}$ is as follows:

$$\alpha = \lim_{M \to \infty} (M + \varepsilon)\left(\frac{\Phi_M}{\Phi_{M-1}} - 1\right). \tag{3.13}$$

The limiting process was facilitated with the VBS algorithm. Columns 2, 3 and 4 of table 1, and figure 3, show $\eta(x)$ determined in this way from the quantities χ_M and $\mathcal{M}_M$ defined in (3.10)-(3.12). There is excellent agreement between the methods in the value of $\eta(x)$.

3.3. Conformal invariance

For the Hamiltonian version of the system the critical anomaly and some of the system's exponents can be found from conformal invariance but there is the added complication of an undetermined parameter ζ: the normalisation factor of the Hamiltonian. This factor ζ arises because any scalar multiple of the Hamiltonian commutes with the transfer matrix and is thus a candidate Hamiltonian for the model. To proceed one must know one of: c; ζ; or a relevant critical exponent.

Table 1. Estimates of η, estimates of the 'energy operator dimension' and estimates of ζ, the normalisation factor of the Hamiltonian. η^a, η^b and η^c are obtained via (3.8) and (3.9) with η^a and η^b defined from the susceptibility χ as in (3.10) and (3.11) respectively, and η^c defined from the magnetisation $\mathcal{M}$ defined in (3.12). η^{wc} is from the weak-coupling expansion (A2.10). The Δ are determined from the method outlined in § 3.3. The ζ are the normalisation factors of the Hamiltonian. ζ^a is determined numerically as described in § 3.3 and ζ^{wc} is from the weak-coupling expansion (A2.9). The error in the data is of the order of the last figure shown.

x	η^a	η^b	η^c	$2\Delta_{01}$	$2\Delta_{23}$	η^{wc}	Δ_{02}	Δ_{13}	ζ^a	ζ^{wc}
1.8	0.229	0.179	0.229	0.231			1.85	1.99	1.52	
1.9	0.216	0.180	0.215	0.216			1.8	1.99	1.57	
2.0	0.205	0.201	0.204	0.205			2.0	2.00	1.62	
2.1	0.197	0.196	0.196	0.197			2.0	2.01	1.67	
2.2	0.190	0.190	0.189	0.189			1.98	2.02	1.72	
2.3	0.183	0.182	0.182	0.183			1.99	2.02	1.77	
2.4	0.178	0.177	0.177	0.178			2.00	2.02	1.82	
2.5	0.173	0.171	0.172	0.173			2.02	2.02	1.86	
2.6	0.168	0.167	0.168	0.169			2.04	2.01	1.91	
2.7	0.164	0.161	0.164	0.164			2.0	2.01	1.95	
2.8	0.160	0.157	0.160	0.161	0.18		2.2	2.01	2.00	
2.9	0.157	0.153	0.157	0.157	0.17		2.3	2.01	2.04	
3.0	0.154	0.152	0.153	0.154	0.16	0.130	2.3	2.02	2.08	2.45
3.1	0.151	0.146	0.150	0.150	0.157	0.128	2.3	2.10	2.12	2.49
3.2	0.148	0.144	0.148	0.148	0.153	0.126	2.2	2.02	2.16	2.53
3.3	0.145	0.140	0.145	0.145	0.150	0.124	2.2	2.01	2.20	2.57
3.4	0.143	1.138	0.143	0.142	0.146	0.122	2.1	2.01	2.24	2.61
3.5	0.141	0.137	0.140	0.140	0.143	0.120	2.1	2.01	2.28	2.65
3.6	0.139	0.133	0.138	0.137	0.140	0.119	2.08	2.02	2.32	2.68
3.7	0.137	0.132	0.136	0.135	0.137	0.117	2.06	2.02	2.36	2.72
3.8	0.135	0.130	0.135	0.133	0.135	0.115	2.05	2.01	2.40	2.76
3.9	0.133	0.129	0.133	0.131	0.133	0.114	2.05	2.01	2.43	2.79
4.0	0.132	0.127	0.132	0.129	0.131	0.113	2.04	2.02	2.47	2.83

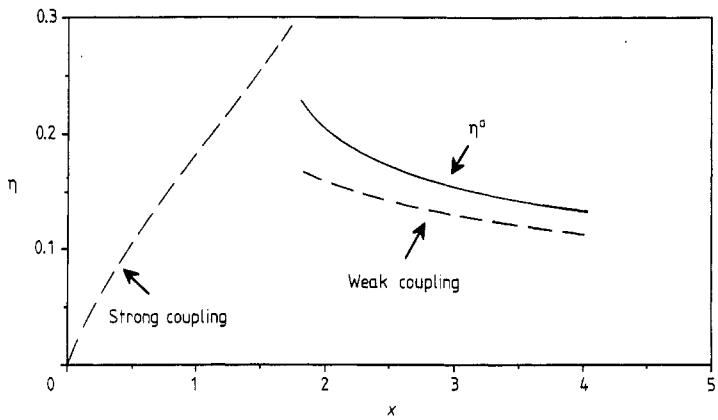

Figure 3. Plots of estimates of the critical index η against coupling x. The plots shown are of η^a from table 1 (which were obtained from the susceptibility χ in (3.10)) and the weak- and strong-coupling expansions (described in §§3.4 and 3.5). The other estimates of η in table 1 (η^b, η^c, $2\Delta_{01}$ and $2\Delta_{23}$) are not shown as they are within a few per cent of η^a.

One expects to find $c = 1$ for the O(2) model. This is because the O(2) model has a scale invariant line of criticality with continuously varying exponents which is only allowed for in models with $c \geqslant 1$. (The factor ζ can be found for those models where the dispersion relation can be determined since the conformally invariant Hamiltonian has the dispersion relation $E \sim p$. However the dispersion relation has not been found for the O(2) model.)

We have derived the critical exponents, assuming $c = 1$, which we compare with those obtained in § 3.2 from finite-size scaling. The comparison is then a test of the $c = 1$ hypothesis.

Specifically Cardy has shown

$$\frac{\omega_0(M)}{M} \sim e_\infty - \frac{\pi \zeta_M c}{6M^2} \tag{3.14}$$

$$F_{ij} \sim \frac{A_{ij}(M)}{M} = \frac{2\pi \zeta_M \Delta_{ij}}{M} \tag{3.15}$$

where e_∞ is the bulk ground-state energy per site, and Δ_{ij} is the anomalous dimension corresponding to the operator connecting states $\|i\rangle\rangle$ and $\|j\rangle\rangle$.

Using data from pairs of lattice sizes, we can extract ζ_M from (3.14). These lattice-dependent ζ_M are extrapolated to the bulk limit ζ. Using (3.15) the $A_{ij}(M)$ are determined and extrapolated to the $M = \infty$ value $A_{ij}(\infty)$. The Δ_{ij} are then found from the ratio $A_{ij}(\infty)/\zeta$.

We expect $2\Delta_{01} = 2\Delta_{23} = \eta$ since the states $\|0\rangle\rangle$ and $\|1\rangle\rangle$ (and the states $\|2\rangle\rangle$ and $\|3\rangle\rangle$) are connected via the magnetic operator. Also we expect $\Delta_{02} = \Delta_{13} = 2$ as this is the dimension corresponding to the energy operator in the critical region (see Cardy 1987). The values of $2\Delta_{01}$, $2\Delta_{23}$, Δ_{02} and Δ_{13} for couplings $x = 1.8$ to 4.0 are listed in table 1. From this table one can see that to within errors $2\Delta_{01} = 2\Delta_{23} = \eta$ as expected and for the interval $x \geqslant 2$ $\Delta_{02} = \Delta_{13} = 2$ within errors. Figure 3 also plots $2\Delta_{01}$ and $2\Delta_{23}$ against x.

These results confirm the identification of the O(2) model as a $c = 1$ conformal system.

3.4. Exponent η as a function of coupling

Our results for the index η can be compared with some theoretical expectations:

(a) As $T \to 0$ (or $x \to \infty$), the low-temperature series analysis of Luck (1982) predicts for the Euclidean version of the model

$$\eta(T) \underset{T \to 0}{\sim} T/2\pi. \tag{3.16}$$

A weak-coupling analysis of the Hamiltonian version of the model outlined in appendix 2 gives an entirely equivalent result

$$\eta(x) \underset{x \to \infty}{\sim} \frac{1}{\pi\sqrt{2x}}. \tag{3.17}$$

The weak-coupling prediction (3.17) is plotted in figure 3. The data appear quite consistent with this asymptotic behaviour.

(b) As $T \to T_c^+$, the renormalisation group analysis of Kosterlitz (1974) predicted

$$\eta(T) \underset{T \to T_c}{\sim} \tfrac{1}{4} - \alpha(T_c - T)^{1/2} \tag{3.18}$$

or in terms of the coupling x

$$\eta(x) \underset{x\to x_c}{\sim} \tfrac{1}{4} - \alpha'(x - x_c)^{1/2}. \tag{3.19}$$

The result $\eta(x_c) = \frac{1}{4}$ is thought to be exact (Nienhuis 1982). Our results do not agree with this prediction, remaining below $\eta = \frac{1}{4}$ to within the estimated errors throughout the region $x = 1.8$–2.0 where the critical point may lie. This might be because $\eta(x_c)$ is not exactly $\frac{1}{4}$; but we believe the more likely explanation is the presence of logarithmic corrections to scaling at the critical point. Such logarithmic corrections are known to occur in the case of the *XXZ* Heisenberg model (Alcaraz *et al* 1987) which is a soluble model with a Kosterlitz-Thouless transition. They render the convergence of the finite lattice results very slow in the vicinity of the transition point, with a corresponding decrease in accuracy of the estimated exponent.

3.5. High-temperature series data

There are some 'high-temperature' series data available for the (1+1)D O(2) model. Series for the mass gap were given by Hamer *et al* (1979) and for the susceptibility by Hamer and Kogut (1979). The series for the mass gap was subsequently extended to tenth order by Hornby and Barber (1985), who used Padé techniques to estimate $x_c = 1.78 \pm 0.06$ and $\sigma = 0.50 \pm 0.08$. The susceptibility series has also been extended recently to eighth order (Guttmann *et al* 1988) (see table 2). Padé analysis of this series assuming a Kosterlitz-Thouless singularity gives $x_c = 1.86 \pm 0.06$.

Table 2. Series coefficients for the ground-state energy per site (ω_0/M), the susceptibility χ and the mass gap F.

Order	ω_0/M	χ	F
0	0	4	1
1	0	16	−2
2	−1	41.6	0.5
3	0	92.4	0.25
4	0.104 166 666 667	185.307 784 857	0.230 208 333 3
5	0	345.121 532 032	0.192 065 972 2
6	0.078 108 465 608 5	613 033 377 144	0.014 473 579 4
7	0	1045.885 044 24	0.089 062 289 4
8	0.004 641 517 200 22	1727.235 404 87	−0.044 807 115 8

Hamer and Kogut (1979) also outlined a way to estimate the critical exponent η using these data. They formed the quantity

$$-\frac{D\log\chi}{D\log F} \underset{g\to g_c}{\sim} 2 - \eta \tag{3.20}$$

using (3.8) and (3.9), and estimated it using Padé approximants†. Using this relationship to define the quantity η in the high-temperature regime, some Padé approximants

† Hamer and Kogut (1979) plotted a curve for the [3,3] approximant, from which they estimated $\eta = 0.26 \pm 0.03$ at g_c, in good agreement with the Kosterlitz prediction $\eta = \frac{1}{4}$. Unfortunately, the length of their series was not sufficient to justify forming a [3, 3] approximant; and our corrected results do not agree with the predictions nearly so well.

obtained from the extended series are shown in figure 3. Again, the results do not agree with the prediction $\eta(x_c) = \frac{1}{4}$. This is not unexpected, since the Padé approximants will not be able to mimic a singular, cusp-like behaviour such as (3.19) in the vicinity of the transition point.

4. Conclusions

Hamiltonian finite-size scaling methods have been applied to the $(1+1)$D O(2) model. Results have been extended from previous work by the study of different schemes for truncating the infinite Hilbert space of configurations into a soluble, finite parcel, by the application of the theory of conformal invariance to the system and by the determination of the critical exponent η. A numerically efficient vector algorithm has been developed for the 'core' routine in the eigensolution package. This routine involves the multiplication of the sparse Hamiltonian matrix by 'Lanczos' vectors in the eigensolution package (see appendix 1).

The hypothesis that the O(2) model falls in conformal invariance class $c = 1$ has been nicely verified by the data. Normalising to this hypothesis, the finite-size scaling amplitudes give values for η in excellent agreement with other estimates and a scaling dimension $\Delta = 2$ for the energy operator, within errors.

The exact position of the Kosterlitz-Thouless transition is difficult to determine accurately due to the exponential decay of the mass gap as $x \to x_c$. From the finite lattice results, we obtained $x_c = 1.9 \pm 0.1$ using the scaled mass gap ratios, $x_c = 2.06 \pm 0.04$ using the Roomany-Wyld β functions, and $x_c = 2.00 \pm 0.03$ using the Romberg mass gap extrapolations (in agreement with the value $x_c = 2.02 \pm 0.02$ obtained by Beleznay (1986)). The high-temperature series analyses give a lower figure, around $x_c = 1.8$. Thus the exact value of x_c remains uncertain to within several per cent. (This is comparable with the situation in the Euclidean version of the model where Monte Carlo estimates have been found to agree on T_c within 10% (Fernández *et al* 1986, Van Himbergen 1984).) All the evidence is in accord with the expected line of critical behaviour for $x > x_c$. The value of $\sigma = 0.501 \pm 0.005$ has been found using the Roomany-Wyld β-function fitting procedure in excellent agreement with the Kosterlitz value of $\sigma = \frac{1}{2}$.

The index η has been estimated as a function of x by several different methods, which are all in excellent agreement. The scaling relations $\tilde{\gamma} = 2 - \eta$ and $\tilde{\beta} = \eta/2$ have been thereby confirmed for this model. In the low-temperature region, our results agree well with the expected asymptotic behaviour $\eta(x) \propto x^{-1/2}$. But near the transition point, they do not agree with the value $\eta(x_c) = \frac{1}{4}$ predicted by Kosterlitz. We believe that this is due to logarithmic corrections to scaling, similar to those occurring in the *XXZ* Heisenberg model.

Acknowledgments

We would like to acknowledge helpful conversations with Professor Michael Barber. We are also very grateful for assistance from the CSIRO Computing Grants Scheme, which allowed us to use the CSIRO Cyber 205 computer. The work of CRA has been supported by a Commonwealth Postgraduate Research Award.

Appendix 1. Numerical details

The program used to set up the Hamiltonian matrix and solve for the energy eigensolutions totals around 1000 lines of FORTRAN code. A Digital VAX computer is used for the 1-7 site calculations and the 8 and 9 site lattice data are from a Cyber 205 supercomputer with a code optimised for vector efficiency. Table 3 illustrates the rapid growth in computing power and storage requirements that are involved as the lattice size increases.

Table 3. Computer used, energy 'cutoff' applied, dimension of arrays, CPU time taken and accuracy of eigenvalues attained for lattice sizes 7, 8 and 9 for the $\langle S \rangle = 0$ sector.

M	Machine	Energy 'cutoff'	Dimension of Hamiltonian	Number of non-zero matrix elements	CPU time taken forming		Accuracy of eigenvalue (at $x = 2.0$)
					Matrix	One eigen-solution	
7	VAX 780	60 units	16 026	106 316	~2000 s	~700 s	one part in 10^9
8	Cyber 205	40 units	23 943	290 000	~28 s	~3 s	one part in 10^7
9	Cyber 205	30 units	34 891	440 000	~92 s	~6 s	one part in 10^5

The barrier to moving to still larger lattices on the Cyber 205 is memory limitations, not excessive CPU time. The total memory needed for a nine-site lattice with a basis state energy cutoff of 30 units exceeds the main memory of the machine. Page faulting becomes by far the dominant component of the nominal cost of the machine and thus limits the size of lattices that can be handled.

The Hamiltonian matrix for the largest sizes studied has dimension 60 000 but is so sparse that it only contains around 700 000 non-zero matrix elements. The 'core' routine in the nested Lanczos algorithm involves the multiplication of this sparse matrix by the 'Lanczos' vectors (see the appendix of Hamer and Johnson (1986)). By using 'gather' and 'scatter' routines a vectorised algorithm has been found for this sparse matrix multiplication which manipulates long vectors, and thus exploits the full speed of the Cyber 205.

An attempt was made to lessen the impact of the truncation of the set of strong-coupling basis states in a 'healing algorithm'. This allows for, in an approximate manner, those strong-coupling states which lie outside the basis state sample but which are connected via $\boldsymbol{V}$ to states inside the sample.

To do this we use the fact that amplitudes $\langle\langle i \| \tilde{\boldsymbol{H}} | I \rangle$ between eigenstates $\| i \rangle\rangle$ and strong-coupling basis states $|I\rangle$ fall off roughly as $\sim e^{-\alpha E^0(I)}$. This gives us approximately the value of amplitude $\langle\langle i \| \tilde{H} | I \rangle_{\text{outside}}$ where $|I\rangle_{\text{outside}}$ is a strong coupling state outside the sample. This can then be used to make corrections to the fully truncated Hamiltonian. However we did not proceed with this method as there is only a slight improvement in the eigenvalues' accuracy, which is not commensurate with the programming complications required.

Appendix 2. Weak-coupling results

Here we derive the first terms in the weak-coupling expansions for $\eta(x)$ and $\zeta(x)$. We

begin the derivation with the Hamiltonian

$$\tilde{H} = \sum_{m=1}^{M} (J^2(m) - x\cos\{\theta(m) - \theta(m+1)\}) \tag{A2.1}$$

(see Hamer *et al* 1979). In the weak-coupling limit ($x \to \infty$) the cosine term becomes dominant. Converting to momentum-space variables:

$$\tilde{\theta}_p = \frac{1}{\sqrt{M}} \sum_{m=1}^{M} \theta_m \, e^{-ipm} \tag{A2.2}$$

with

$$p = \frac{2\pi n}{M} \qquad n = \begin{cases} \left\{\dfrac{-(M-2)}{2}, \ldots, 0, \ldots, \dfrac{M}{2}\right\} & M \text{ even} \\ \left\{\dfrac{-(M-1)}{2}, \ldots, 0, \ldots, \dfrac{M-1}{2}\right\} & M \text{ odd} \end{cases} \tag{A2.3}$$

and with a change of variables one finds that the Hamiltonian can be written in a diagonal form corresponding to a sum of harmonic oscillators each with energy

$$E_p = (n_p + \tfrac{1}{2})\omega_p \tag{A2.4a}$$

$$\omega_p = 2[x(1-\cos p)]^{1/2}. \tag{A2.4b}$$

Hence as $M \to \infty$ the dispersion relation for fundamental excitations becomes

$$E(p) \underset{M\to\infty}{\sim} \sqrt{2x}\, p. \tag{A2.5}$$

The mass gap has been argued by Hamer and Barber (1981) to be

$$F_M \underset{M\to\infty}{\sim} \frac{1}{M}. \tag{A2.6}$$

Comparing (A2.5) and (A2.6) with the formulae predicted by conformal invariance

$$E(p) \sim \zeta p \tag{A2.7}$$

$$F_M \sim \frac{\pi\zeta\eta}{M} \tag{A2.8}$$

gives

$$\zeta = \sqrt{2x} \tag{A2.9}$$

and

$$\eta = \frac{1}{\pi\sqrt{2x}} \tag{A2.10}$$

in the weak-coupling limit†. The values of $\zeta(x)$ determined numerically in § 3.3 are compared with the weak-coupling behaviour (A2.9) in table 1. Figure 3 includes a plot of the behaviour of $\eta(x)$ in the weak-coupling limit (from A2.10)).

† This result exactly matches the Euclidean formula $\eta = T/2\pi$ predicted by Luck (1982), given the correspondences $x = 2/g^2$ and $g = T$ (Hamer *et al* 1979).

References

Alcaraz F C, Barber M N and Batchelor M T 1987 *Phys. Rev. Lett.* **58** 771
Barber M N and Hamer C J 1982 *J. Aust. Math. Soc.* B **23** 229
Belavin A A, Polyakov A M and Zamolodchikov A B 1984a *J. Stat. Phys.* **34** 763
—— 1984b *Nucl. Phys.* B **241** 333
Beleznay F 1986 *J. Phys. A: Math. Gen.* **19** 551
Berger W A, Miller H G, Kreuzer K-G and Dreizler R M 1977 *J. Phys. A: Math. Gen.* **10** 1089
Cardy J L 1987 *Phase Transitions and Critical Phenomena* vol 11, ed C Domb and J L Lebowitz (New York: Academic) p 55
Fernández J F, Ferreira M F and Stankiewicz J 1986 *Phys. Rev.* B **34** 292
Guttmann A J, Hamer C J and Burden C J 1988 in preparation
Hamber H W and Richardson J L 1981 *Phys. Rev.* B **23** 4698
Hamer C J 1982 *J. Phys. A: Math. Gen.* **15** L675
Hamer C J and Barber M N 1980 *J. Phys. A: Math. Gen.* **13** L169
—— 1981 *J. Phys. A: Math. Gen.* **14** 259
Hamer C J and Kogut J B 1979 *Phys. Rev.* B **20** 3859
Hamer C J, Kogut J B and Susskind L 1979 *Phys. Rev.* D **19** 3091
Hamer C J and Johnson C H J 1986 *J. Phys. A: Math. Gen.* **19** 423
Heys D W and Stump D R 1984 *Phys. Rev.* D **29** 1784
Hornby P G and Barber M N 1985 *J. Phys. A: Math. Gen.* **18** 827
Irving A C and Hamer C J 1983 *J. Phys. A: Math. Gen.* **16** 829
Kosterlitz J M 1974 *J. Phys. C: Solid State Phys.* **7** 1046
Kosterlitz J M and Thouless D J 1973 *J. Phys. C: Solid State Phys.* **6** 1181
Lubkin S 1952 *J. Res. Nat. Bur. Standards* **48** 228
Luck J M 1982 *J. Phys. A: Math. Gen.* **15** L169
Mattis D C 1984 *Phys. Lett.* **104A** 357
Migdal A A 1975 *Zh. Eksp. Teor. Fiz.* **69** 1457 (Engl. transl. 1975 *Sov. Phys.-JETP* **42** 743)
Nienhuis B 1982 *Phys. Rev. Lett.* **49** 1062
Patkós A and Ruján P 1985 *J. Phys. A: Math. Gen.* **18** 1765
Pesch W and Kroemer J 1985 *Z. Phys.* B **59** 317
Polyakov A 1970 *Zh. Eksp. Teor. Fiz. Pis. Red.* **12** 538 (Engl. transl. 1970 *JETP Lett.* **12** 381)
Roomany H H and Wyld H W 1980 *Phys. Rev.* D **21** 3341
Stump D R 1980 *Phys. Rev.* D **22** 2490
—— 1986 *Nucl. Phys.* B **265** [FS15] 113
Vanden Broeck J-M and Schwartz L W 1979 *SIAM J. Math. Anal.* **10** 658
Van Himbergen J E 1984 *J. Phys. C: Solid State Phys.* **17** 5039